Single beam grating coupled interferometry: high resolution miniaturized label-free sensor for plate based parallel screening

Daniel Patko,[1,2] Kaspar Cottier,[3] Andras Hamori,[1] and Robert Horvath[1*]

[1] *Research Institute for Technical Physics and Material Science MFA Hungarian Academy of Sciences, H-1120 Konkoly-Thege út 29-33, Budapest, Hungary*

[2] *Doctoral School of Molecular- and Nanotechnologies, Faculty of Information Technology, University of Pannonia; H-8200 Egyetem u.10, Veszprém, Hungary*

[3] *Creoptix GmbH Einsiedlerstrasse 25 CH-8820 Waedenswil, Switzerland*

**horvathr@mfa.kfki.hu*

Abstract: Grating Coupled Interferometry (GCI) using high quality waveguides with two incoupling and one outcoupling grating areas is introduced to increase and precisely control the sensing length of the device; and to make the sensor design suitable for plate-based multiplexing. In contrast to other interferometric arrangements, the sensor chips are interrogated with a single expanded laser beam illuminating both incoupling gratings simultaneously. In order to obtain the interference signal, only half of the beam is phase modulated using a laterally divided two-cell liquid crystal modulator. The developed highly symmetrical arrangement of the interferometric arms increases the stability and at the same time offers straightforward integration of parallel sensing channels. The device characteristics are demonstrated for both TE and TM polarized modes.

OCIS codes: (280.0280) Remote sensing and sensors; (050.0050) Diffraction and gratings.

References and Links

1. J. J. Ramsden, *Biomedical Surfaces* (Artech House, 2007).
2. M. Malmsten, *Biopolymers at Interfaces* (Taylor & Francis, 2003).
3. J. M. Coles, D. P. Chang, and S. Zauscher, "Molecular mechanisms of aqueous boundary lubrication by mucinous glycoproteins," Curr. Opin. Coll. Int. Sci. **15**(6), 406–416 (2010).
4. M. A. Cooper, "Optical biosensors in drug discovery," Nat. Rev. Drug Discov. **1**(7), 515–528 (2002).
5. Y. Fang, "Label-free receptor assays," Drug Discov. Today. Technol. **7**(1), 5–11 (2010).
6. C. Calonder and P. R. Van Tassel, "Kinetic regimes of protein adsorption," Langmuir **17**(14), 4392–4395 (2001).
7. J. J. Ramsden, "Review of new experimental methods for investigating random sequential adsorption," J. Stat. Phys. **73**(5-6), 853–877 (1993).
8. E. K. Mann, L. Heinrich, and P. Schaaf, "Validation of the uniform thin-film approximation for the optical analysis of particulate films," Langmuir **13**(18), 4906–4909 (1997).
9. X. Fan, I. M. White, S. I. Shopova, H. Zhu, J. D. Suter, and Y. Sun, "Sensitive optical biosensors for unlabeled targets: a review," Anal. Chim. Acta **620**(1-2), 8–26 (2008).
10. H. K. Hunt and A. M. Armani, "Label-free biological and chemical sensors," Nanoscale **2**(9), 1544–1559 (2010).
11. Y. Fang, A. M. Ferrie, N. H. Fontaine, J. Mauro, and J. Balakrishnan, "Resonant waveguide grating biosensor for living cell sensing," Biophys. J. **91**(5), 1925–1940 (2006).
12. J. J. Ramsden and R. Horvath, "Optical biosensors for cell adhesion," J. Recept. Signal Transduct. Res. **29**(3-4), 211–223 (2009).
13. R. Horvath, K. Cottier, H. C. Pedersen, and J. J. Ramsden, "Multidepth screening of living cells using optical waveguides," Biosens. Bioelectron. **24**(4), 799–810 (2008).
14. J. Homola, S. S. Yee, and G. Gauglitz, "Surface plasmon resonance sensors: review," Sens. Actuators B Chem. **54**(1-2), 3–15 (1999).
15. V. B. Braginsky, M. L. Gorodetsky, and V. S. Ilchenko, "Quality factor and nonlinear properties of optical whispering Gallery modes," Phys. Lett. A **137**(7-8), 393–397 (1989).
16. N. Skivesen, A. Têtu, M. Kristensen, J. Kjems, L. H. Frandsen, and P. I. Borel, "Photonic-crystal waveguide biosensor," Opt. Express **15**(6), 3169–3176 (2007).
17. V. N. Konopsky and E. V. Alieva, "A biosensor based on photonic crystal surface waves with an independent registration of the liquid refractive index," Biosens. Bioelectron. **25**(5), 1212–1216 (2010).
18. N. Skivesen, R. Horvath, and H. C. Pedersen, "Optimization of metal-clad waveguide sensors," Sens. Actuators B Chem. **106**(2), 668–676 (2005).

#170857 - $15.00 USD Received 22 Jun 2012; revised 6 Sep 2012; accepted 7 Sep 2012; published 24 Sep 2012

19. N. Skivesen, R. Horvath, S. Thinggaard, N. B. Larsen, and H. C. Pedersen, "Deep-probe metal-clad waveguide biosensors," Biosens. Bioelectron. **22**(7), 1282–1288 (2007).
20. W. Lukosz, "Integrated optical chemical and direct biochemical sensors," Sens. Actuators B Chem. **29**(1-3), 37–50 (1995).
21. K. Tiefenthaler and W. Lukosz, "Sensitivity of grating couplers as integrated-optical chemical sensors," J. Opt. Soc. Am. B **6**(2), 209–220 (1989).
22. J. Vörös, J. J. Ramsden, G. Csúcs, I. Szendro, S. M. De Paul, M. Textor, and N. D. Spencer, "Optical grating coupler biosensors," Biomaterials **23**(17), 3699–3710 (2002).
23. C. Picart, C. Gergely, Y. Arntz, J. C. Voegel, P. Schaaf, F. J. G. Cuisinier, and B. Senger, "Measurement of film thickness up to several hundreds of nanometers using optical waveguide lightmode spectroscopy," Biosens. Bioelectron. **20**, 553–561 (2004).
24. M. M. Abadla, M. M. Shabat, and D. Jäger, "Simulation of sensing characteristics in optical nonlinear waveguide sensors," Laser Phys. **14**, 1231–1237 (2004).
25. S. A. Taya, M. M. Shabat, and H. M. Khalil, "Nonlinear planar asymmetrical optical waveguides for sensing applications," Optik (Stuttg.) **121**(9), 860–865 (2010).
26. B. A. Forbes, D. F. Sahm, and A. S. Weissfeld, *Diagnostic Microbiology* (Mosby, 1998), Chap. 15.
27. W. Lukosz, P. M. Nellen, C. Stamm, and P. Weiss, "Output grating couplers on planar wave-guides as integrated optical chemical sensors," Sens. Actuators B Chem. **1**(1-6), 585–588 (1990).
28. K. Schmitt, B. Schirmer, C. Hoffmann, A. Brandenburg, and P. Meyrueis, "Interferometric biosensor based on planar optical waveguide sensor chips for label-free detection of surface bound bioreactions," Biosens. Bioelectron. **22**(11), 2591–2597 (2007).
29. P. K. Tien, "Integrated optics and new wave phenomena," Rev. Mod. Phys. **49**(2), 361–420 (1977).
30. N. Aggarwal, K. Lawson, M. Kershaw, R. Horvath, and J. J. Ramsden, "Protein adsorption on heterogeneous surfaces," Appl. Phys. Lett. **94**(8), 083110 (2009).
31. J. Dübendorfer and R. E. Kunz, "Compact integrated optical immunosensor using replicated chirped grating coupler sensor chips," Appl. Opt. **37**(10), 1890–1894 (1998).
32. B. Agnarsson, A. B. Jonsdottir, N. B. Arnfinnsdottir, and K. Leosson, "On-chip modulation of evanescent illumination and live-cell imaging with polymer waveguides," Opt. Express **19**(23), 22929–22935 (2011).
33. R. Horvath, L. R. Lindvold, and N. B. Larsen, "Fabrication of all-polymer freestanding waveguides," J. Micromech. Microeng. **13**(3), 419–424 (2003).
34. R. Horvath, H. C. Pedersen, N. Skivesen, C. Svanberg, and N. B. Larsen, "Fabrication of reverse symmetry polymer waveguide sensor chips on nanoporous substrates using dip-floating," J. Micromech. Microeng. **15**(6), 1260–1264 (2005).
35. R. Horvath, H. C. Pedersen, and N. B. Larsen, "Demonstration of reverse symmetry waveguide sensing in aqueous solutions," Appl. Phys. Lett. **81**(12), 2166–2168 (2002).
36. R. Horváth, H. C. Pedersen, N. Skivesen, D. Selmeczi, and N. B. Larsen, "Optical waveguide sensor for on-line monitoring of bacteria," Opt. Lett. **28**(14), 1233–1235 (2003).
37. R. Horvath, H. C. Pedersen, N. Skivesen, D. Selmeczi, and N. B. Larsen, "Monitoring of living cell attachment and spreading using reverse symmetry waveguide sensing," Appl. Phys. Lett. **86**(7), 071101 (2005).
38. R. Horvath, H. C. Pedersen, and F. J. G. Cuisinier, "Guided wave sensing of polyelectrolyte multilayers," Appl. Phys. Lett. **88**(11), 111102 (2006).
39. R. E. Kunz and K. Cottier, "Optimizing integrated optical chips for label-free (bio-)chemical sensing," Anal. Bioanal. Chem. **384**(1), 180–190 (2006).
40. E. K. Mann, "Evaluating optical techniques for determining film structure: Optical invariants for anisotropic dielectric thin films," Langmuir **17**(19), 5872–5881 (2001).
41. R. Horvath, J. McColl, G. E. Yakubov, and J. J. Ramsden, "Structural hysteresis and hierarchy in adsorbed glycoproteins," J. Chem. Phys. **129**(7), 071102 (2008).
42. The home page of the Microvacuum (Microvacuum 2012) *http://www.microvacuum.com*
43. The home page of the Corning (Corning 2012) *http://www.corning.com/lifesciences/us_canada/en/whats_new/epic_system.aspx*
44. The home page of the SRU Biosystems. (SRU Biosystems 2012) *http://www.srubiosystems.com/*
45. C. J. Choi and B. T. Cunningham, "Single-step fabrication and characterization of photonic crystal biosensors with polymer microfluidic channels," Lab Chip **6**(10), 1373–1380 (2006).
46. A. Mashaghi, M. Swann, J. Popplewell, M. Textor, and E. Reimhult, "Optical anisotropy of supported lipid structures probed by waveguide spectroscopy and its application to study of supported lipid bilayer formation kinetics," Anal. Chem. **80**(10), 3666–3676 (2008).
47. The home page of the Farfield Group. (Farfield Group 2012) *http://www.farfield-group.com/*
48. P. Kozma, A. Hamori, K. Cottier, S. Kurunczi, and R. Horvath, "Grating coupled interferometry for optical sensing," Appl. Phys. B **97**(1), 5–8 (2009).
49. P. Kozma, A. Hamori, S. Kurunczi, K. Cottier, and R. Horvath, "Grating coupled optical waveguide interferometer for label-free biosensing," Sens. Actuators B Chem. **155**(2), 446–450 (2011).
50. The home page of the Creoptix GmbH. (Creoptix GmbH 2012) *http://www.creoptix.com/*
51. S. Grego, K. H. Gilchrist, J. B. Carlson, and B. R. Stoner, "A compact and multichannel optical biosensor based on a wavelength interrogated input grating coupler," Sens. Actuators B Chem. **161**(1), 721–727 (2012).

#170857 - $15.00 USD Received 22 Jun 2012; revised 6 Sep 2012; accepted 7 Sep 2012; published 24 Sep 2012

1. Introduction

There is an increasing need for cost-effective, reliable and high resolution measurements of biological and chemical processes in the health, biotechnology and military areas. Measuring biomolecular or cellular interactions at the nanometer length scale also opens up several challenging applications in basic biological, chemical and biophysical research with significant industrial relevance [1–6]. It is especially useful when the processes and interactions are monitored without the need of any fluorescent or radioactive labelling; by following, for example, refractive index variations caused by the inherent polarizability of biomolecules [6–10] or living cells [11–13].

This type of label-free optical detection can be exploited by using optical resonances; such as surface plasmons [14], whispering gallery modes [15], photonic crystals [16,17], metal-clad [18,19] and dielectric waveguides [11–13,20–23]. Recently nonlinear optical waveguides for label-free sensing have also been investigated [24,25]. By avoiding any labeling, the state of the molecules or cells under investigation is less affected by the measurement [4,12] and one also decreases the costs associated with a single test. However, today, the above devices fall behind traditional labelling methods like Enzime Linked Immunosorbent Assay (ELISA) [26] in terms of sensitivity, straightforward operation and reputation by the wide scientific and industrial community. In this regard, except the relatively well-known Surface Plasmon Resonance (SPR) sensors [14], the most sensitive and promising label-free optical configurations are still in their infancy.

Integrated optical waveguides are promising candidates to be exploited as miniaturized sensing units. These devices offer higher sensitivity than conventional SPR sensors, especially when combined with optical interferometry [27,28]. The user's applications are not limited to metal surfaces; the waveguides can be coated with almost any type of transparent dielectric material of interest [22,29,30]. Moreover, integrated optical waveguides can be fabricated using cost effective polymer fabrication technology [29,31–34]. Using reverse symmetry waveguides with low refractive index (RI) supports [35], the probing depth of the evanescent field of the waveguide mode can be fitted to the size of the monitored object, which can range from nanometer scale molecules to several micrometer large bacterial [36] or mammalian cells [37]. It is also possible to monitor the deposited biological layers with guided waves instead of evanescent ones. This type of detection has larger dynamic range and better sensitivity compared to evanescent wave sensing [38]. Therefore, the waveguide sensor structure can be tailor made and fitted to a wide range of applications [39]. Moreover, optical waveguides can support several modes with different polarization and probing depth. Multimode waveguide were used to monitor optical birefringence in monlayers of biomolecules [40,41] and to follow refractive index variations in living cells [13].

Several commercial sensors employing planar optical waveguides are already on the market. For example, Optical Waveguide Lightmode Spectroscopy (OWLS) [42] is a well known table top research instrument, while the Corning's EPIC [43] and the SRU's BIND [44] systems offer microplate based high throughput screening (HTS) of molecular and cellular events for industrial applications. The SRU's technology was also demonstrated in lab-on-a chip devices [45]. The above systems are based on angular or wavelength interrogation of grating coupled planar optical waveguides, having lower sensitivities and more limited dynamic range than what would be offered by waveguide based interferometry [8,28,46]; like the commercially available table top DPI (Dual Polarization Interferometry) system [47].

Grating Coupled Interferometry (GCI) is a label-free optical sensing concept introduced by us recently [48,49] and related products will be commercialized by Creoptix GmbH [50]. The innovation combines the cost-effectiveness, simplicity and reliability of grating coupled planar optical waveguides with the excellent resolution of interferometric measurements. In the configuration originally proposed, a planar optical waveguide with an ion-implanted incoupling grating was placed into a Mach-Zehnder type interferometric arrangement. In the previous GCI arrangement [49], two parallel and coherent laser beams were coupled into the

#170857 - $15.00 USD Received 22 Jun 2012; revised 6 Sep 2012; accepted 7 Sep 2012; published 24 Sep 2012

waveguide using a single grating coupler. This way the beams were combined in the waveguide itself creating an interference signal, which was picked up by a suitable detector.In order to phase modulate one of the arms of the interferometer a liquid crystal cell was used. Effective refractive index changes in the waveguide between (and also on) the two incoupling regions were followed by monitoring characteristic changes in the measured interference signal [48,49].

In the present contribution, we demonstrate the great potential in the GCI concept to obtain miniaturized sensor units with remarkable sensitivity in a simple and cost effective way. First, we use waveguides with excellent guiding characteristics in order to increase the sensing length of the device. Moreover, the new waveguide design have two well separated incoupling gratings followed by an outcoupling grating area in order to precisely control the sample interaction length and to completely avoid the need for butt-end detection of GCI signals. Secondly, a novel, simple and reliable interferometric arrangement is also introduced. In this, instead of two separated and parallel beams - which are rather difficult to align - we simply apply a single expanded beam illuminating both incoupling gratings simultaneously. A two-cell liquid crystal modulator is placed in the path of the beam to modulate its phase.This arrangement is not only highly symmetrical, reducing the interferometer's free space noise, but due to the large homogeneously illuminated grating areas makes the integration of parallel sensing channels straightforward. This feature is demonstrated by placing a two-channel cuvette on top of the waveguide and measuring bulk refractive index variations and protein adsorption at the various sensing channels. The performances of TE and TM polarized modes were also compared, both theoretically and experimentally.

All of the above developments make the introduced GCI configuration ideal for plate based, cost-effective label-free sensor array development in miniaturized analytical systems and in industrial High Throughput Screening (HTS) applications; especially where the excellent sensitivity is crucial. Based on the recent improvements, a commercial sensor instrument is being developed by Creoptix.

2. Materials and methods

2.1 Waveguide sensor design

The cross section of the fabricated waveguide sensors (Optics Balzers, Liechtenstein) is schematically shown in Fig. 1(a). The waveguide support is a 1 mm thick glass substrate with refractive index n_s = 1.52 (at 633 nm). In order to fabricate the GCI chips, first, three surface relief gratings were etched into the substrate with approximately 300 nm periodicities. Second, the substrate was covered with a highly compact Ta_2O_5 film with thickness d_F in the range of 130-150 nm and refractive index n_F = 2.12. The role of the 1st and 2nd gratings is to couple the light into the Ta_2O_5 waveguide, while the 3rd grating couples the waveguide mode into free space (see Fig. 1(a)).The second grating acts as miniaturized beam combiner and is therefore shorter by design in order to transmit a significant fraction of the guided mode. In the present GCI configuration, the sample interacts with the modes of the waveguide between the two incoupling grating areas. The whole waveguide surface - except a 5 mm long area between the two incoupling gratings - was covered with a relatively thick layer of SiO_2 (see Fig. (1a)). The thickness of the SiO_2 film was chosen to be thicker than the penetration depth of the mode in the SiO_2 layer. This way the incoupling and outcoupling angles are not affected by sample RI variations, and the sample interaction length (sensing window of the device) is precisely controlled. The evanescent field of the propagating waveguide mode interacts with the sample at the above mentioned 5 mm long area. Refractive index variation inside the SiO_2 opening shifts the phase of the measuring light (which is incoupled at the 1st grating) relative to the phase of the reference light (coupled into the waveguide at the 2nd grating) (see Fig. 1(a)). In this way the measuring and the reference beams of the interferometer are joined in the waveguide itself after the 2nd incoupling grating, creating the interference signal.This intensity signal is coupled into an optical fiber placed under the

#170857 - $15.00 USD Received 22 Jun 2012; revised 6 Sep 2012; accepted 7 Sep 2012; published 24 Sep 2012

outcoupling grating and measured by a suitable detector (see Fig. 1(a)). In a GCI arrangement the measuring light is usually phase modulated (see details later).

The photo of the waveguide chip is shown in Fig. 1(b), demonstrating the excellent guiding characteristics of the fabricated waveguides. It is seen that during the mode propagation from the 2nd incoupling grating to the outcoupling grating no mode damping can be visually observed. This is an improvement over the previously applied waveguides [48,49], where the modes damped in 3-4 mm due to the relatively lower waveguiding quality and the application of a single grating.

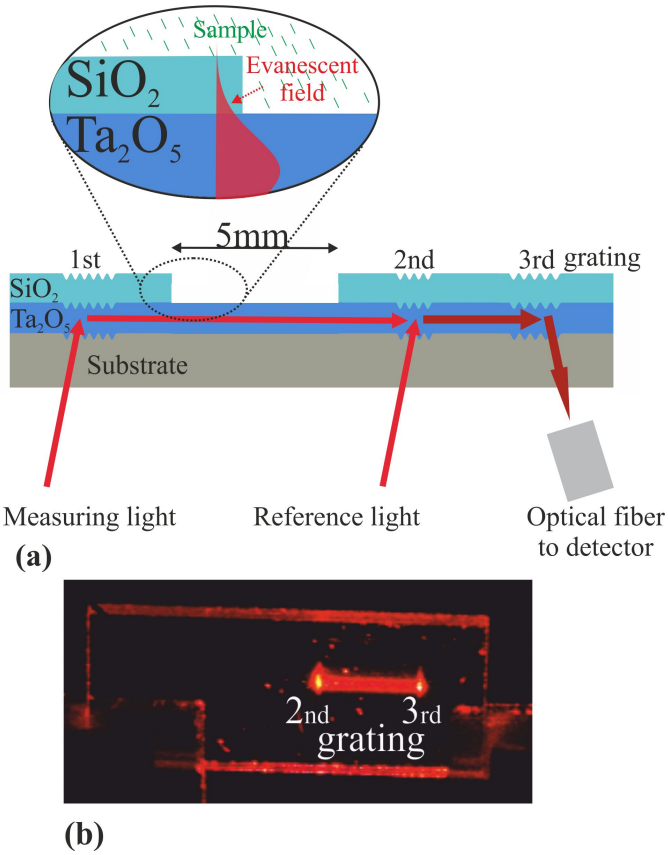

Fig. 1. (a) Cross section of the waveguide sensor. The measuring light is coupled into the waveguide through the first grating. The reference light is incoupled at the second grating. The interfrence signal is outcoupled at the third grating and picked up by a fiber coupled optical detector. The 5 mm long opening in the SiO_2 layer represents the sensing window of the device. (b) Photo of the waveguide chip showing mode propagation between the second incoupling grating and the third outcoupling grating.

2.2 Single beam interferometric configuration

The above described waveguide was placed into the optical arrangement schematically shown in Fig. 2. In this, a 0.8 mm wide He-Ne laser beam (633nm, 5mW, Lasos Lasertechnik GmbH.) was expanded to 1.5 cm using a 30x microscope objective and a suitable collimator lens (see Fig. 2(a)). The resulting beam illuminated the GCI chip through a two-cell liquid crystal modulator (LCM). The expanded beam is wide enough to illuminate both incoupling gratings simultaneously. In order to fulfil the incoupling condition [21,29] at the gratings the waveguide was slightly tilted relative to the beam using a suitable chip holder (not shown in Fig. 2(a), but visible in Fig. 2(b)).

#170857 - $15.00 USD Received 22 Jun 2012; revised 6 Sep 2012; accepted 7 Sep 2012; published 24 Sep 2012

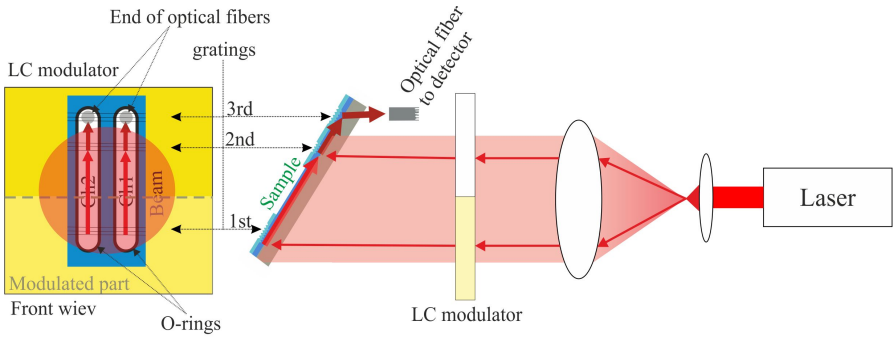

(a)

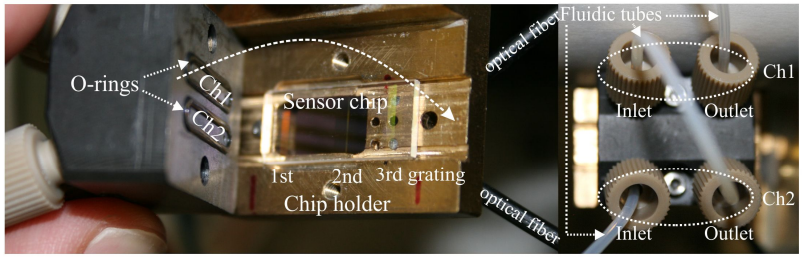

(b)

Fig. 2. (a) Schematic drawing of the optical setup. (b) (left) Photo of the waveguide sensor chip holder and the dual channel flow through cuvette before assembly. The waveguide sensor chip with the three gratings, the O-rings of the fluidic channels and the optical fibers are clearly seen. (right) Top view of the assembled unit. The two fluidic channels are connected in series.

The above arrangement has many advantages over traditional two beam interferometers. First, the application of two parallel beams illuminating the two incoupling gratings is completely avoided. In the new setup, the lower and upper part of the expanded beam (illuminating the 1st and 2nd gratings, respectively) should be considered as the beginning of the two arms of the interferometer (see Fig. 2(a)).This way, the "beams" illuminating the gratings are perfectly parallel without any lengthy alignment, making especially easy to set up the device. Secondly, the developed interferometric arrangement is highly symmetrical. The light waves propagating in the two interferometric arms are passing through the same liquid crystal modulator and travel approximately the same distance in free space. The small difference is caused by the slight tilt of the waveguide (see Fig. 2(a)), which is necessary to satisfy the coupling conditions at the gratings.Therefore, thermal fluctuations and vibrations causing common phase variations in the interferometer are well compensated. Moreover, since the LCM has two separately addressable cells the two arms of the interferometer can be individually phase modulated. In the application presented here the lower half of the beam - which illuminates the 1st incoupling grating in Fig. 2(a) - was phase modulated.

It should be noted that those parts of the expanded beam which do not impinge on any gratings are not coupled into the waveguide, causing some loss of laser power. We found however, that optimizing the width of the expanded Gaussian beam using the separation distance and coupling length of the two incoupling gratings this loss can be minimized, resulting in strong enough interference signals at the photodetector.

2.3 Integration of parallel sensing channels - dual channel flow-through cuvette

The developed single beam interferometric approach has another inportant advantage. The integration of parallel sensing channels is simple and straightforward . This is demonstrated by placing a chemically and mechanically resistant PEEK (Polyether ether ketone) cuvette with two parallel elongated shaped O-rings on top of the waveguide sensor (see Fig. 2(a) and

#170857 - $15.00 USD Received 22 Jun 2012; revised 6 Sep 2012; accepted 7 Sep 2012; published 24 Sep 2012

2(b)). The O-rings not only define the fluidic part of the two sensing channels, but also strongly damp the waveguide mode propagating underneath the O-rings. Therefore, the two sensing channels are optically sealed from each other, avoiding channel to channel interference. The GCI signals of the two channels can be easily picked up by two optical fibers positioned under the outcoupling grating (see Fig. 2(a) and 2(b)). The fibers are fixed in the metal chip holder (Fig. 2(b)) and guide the GCI interference signal to two photodetectors. Using a Peltier based temperature controlling system the metal chip holder was temperature stabilized at 24 °C.

2.4 Sample materials and chemicals

The various sample solutions were flowed through the cuvettes using a 12 roller peristaltic pump (Ismatec Reglo Digital) at flow rate of 2μL/s. In the bulk refractive index measurements various concentrations (0.5%, 1%, 5%) of glycerol (WWR International) dissolved in ultrapure water were applied. Prior to measurements the refractive indices of the samples were measured by a Rudolf refractometer and found to be n_{water} = 1.33055, $n_{0.5\%}$ = 1.33115, $n_{1\%}$ = 1.33207 and $n_{5\%}$ = 1.33676.For the protein adsorption tests fibrinogen from bovine plasma (Sigma, F8630-1G) dissolved in phosphate buffered saline (PBS, Sigma, P4417-100TAB) at a final concentration of 0.1 mg/ml was applied. Fibrinogen has three protein domains; α chain (63.5 kD), β chain (56 kD) and γ chain (47 kD) giving an overall molecular weight of 166.5 kDa. The corresponding bulk refractive indices were n_{Fibr} = 1.33303 and n_{PBS} = 1.33301. The used and contaminated waveguides were cleaned in chromsulfuric acid for 2-3 minutes, rinsed in ultrapure water and after in 0.1 M KOH. The cleaning procedure was finished by an extensive rinsing in ultrapure water.

3. Results and discussion

3.1 Phase modulation and internal referencing

In order to obtain the GCI interference signals, the measuring beam was phase modulated by driving the lower cell of the LCM with a periodical square wave voltage shown in Fig. 3(a) The recorded interference signal during one relaxation period could be well fitted with the following analytical formula for $t_{rel}<\tau$ (see Fig. 3(b)).

$$I(t_{rel}) = I_0 + A\cos\left[\varphi_{LCM} e^{-2t_{rel}/\tau} - \varphi_{LCM} - \phi(t)\right], \quad (1)$$

where A is the signal amplitude, I_0 is the offset of the interference signal, φ_{LCM} is the total phase shift of the LC modulator, τ is the time constant of the relaxation process; and $\phi(t)$ is the phase difference between the measuring and reference arms at time *t*. t_{rel} is the time variable during one relaxation period [49].

In the first experiment, both channel one (Ch1) and channel two (Ch2) were filled up with ultrapure water. Figure 3(b) shows the interference signals recorded in the two channels. It is seen that a typical interference signal has two minimas and maximas proving that the total phase shift at the LCM during the relaxation is above 2π. By periodically recording the interference signals in the two measuring channels and calculating the phase values using Eq. (1), the relative phase shifts caused by the sample can be monitored in real time. By using one of the channels as internal reference, recording only background variations, the performance of the sensor could be significantly increased. The noise of the recorded phase signals was in the range of 10^{-4}- $3x10^{-3}$ radians depending on the actual waveguide and polarization. It is important to note that the present setup has a maximum time resolution of 7 ms, making possible to follow relatively fast processes too.

#170857 - $15.00 USD Received 22 Jun 2012; revised 6 Sep 2012; accepted 7 Sep 2012; published 24 Sep 2012

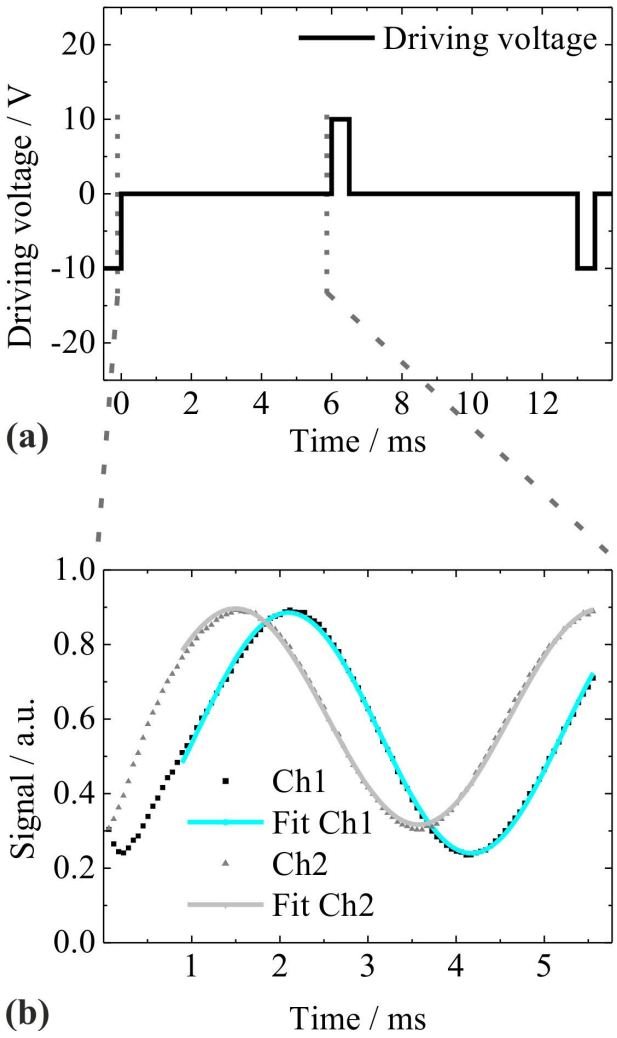

Fig. 3. (a) Driving voltage on the active part of the LCM. (b) The measured interference signals of the two channels (Ch1 and Ch2) during a typical relaxation period of the LCM. The fits of Eq. (1) to the recorded data are also shown (solid lines).

3.2 Theoretical sensitivities of the waveguide modes

In the present section, we calculate the internal sensitivities $\partial N / \partial n_C$ and $\partial N / \partial d_A$ of the fabricated waveguides for the lowest order modes with different polarizations, TE_0 and TM_0. According to Tiefenthaler and Lukosz [21], N is the effective refractive index of the waveguide mode, n_C is the refractive index of the media covering the film and d_A is the thickness of the adlayer deposited on the sensor. $\partial N / \partial n_C$ is the refractive index sensitivity and $\partial N / \partial d_A$ is the adlayer thickness sensitivity of the mode. In the calculations we use n_F = 2.12, n_S = 1.52, n_C = 1.33 and n_A = 1.45 for the refractive index of the waveguide film, substrate, aqueous cover and thin adlayer, respectively.

#170857 - $15.00 USD Received 22 Jun 2012; revised 6 Sep 2012; accepted 7 Sep 2012; published 24 Sep 2012

The fabricated waveguides had a Ta_2O_5 film thickness in the range of 130-155 nm. It is clearly seen that in this range the TM_0 has the highest sensitivity values and the performance of the TE_0 mode is slightly lower (Fig. 4).

Based on the calculated sensitivities of the modes the phase shifts can be determined using the following equations.

$$\Delta\phi = kL\frac{\partial N}{\partial n_C}\Delta n_C. \tag{2}$$

$$\Delta\phi = kL\frac{\partial N}{\partial d_A}\Delta d_A. \tag{3}$$

where k ($k = 2\pi/\lambda$, $\lambda = 633$ nm wavelength of the measuring light) is the vacuum wave vector, L is the sensing length (5 mm in the present case).

Taking the maximum theoretical sensitivity values of the TM_0 mode and the above measured lowest possible phase noise (10^{-4} radians) it can be easily calculated using Eq. (2) and Eq. (3) that this phase noise corresponds to a sample refractive index change of 10^{-8}, and $4x10^{-6}$ nm change in adlayer thickness.

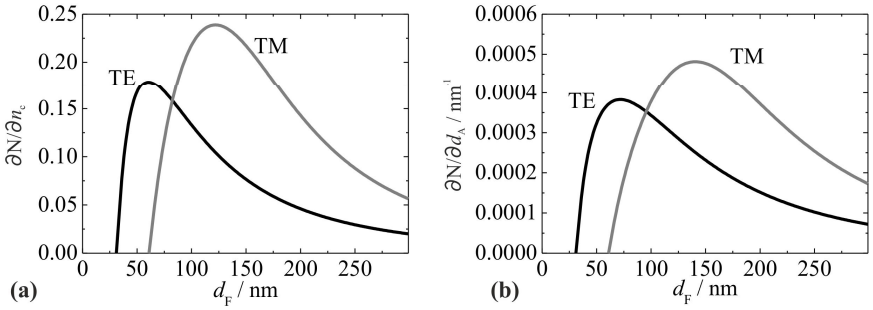

Fig. 4. Theoretical sensitivities of the waveguide sensor structure plotted in the function of waveguide film thickness. (a) Refractive index sensitivity. (b) Adlayer thickness sensitivity.

3.3Refractive index sensing and lateral homogeneity of the fabricated waveguides

In order to evaluate the performance of the new configuration, the following experiment was carried out for both polarizations. In this the two fluidic channels were connected in series (see Fig. 2(b)). First, pure water was pumped into the channels with a constant flow rate, followed by various glycerol solutions and ultrapure water in between (see Fig. 5). It is clearly seen that for the same refractive index variation the configuration using TM polarization gave phase shifts more than three times than that of the TE. Keeping in mind the refractive indices of the solutions the calculated bulk sensitivity values were 0.2346 for TM and 0.074 for TE, which is in excellent agreement with the theoretical calculations depicted in Fig. 4 for the above mentioned thickness range of the waveguides.

The linearity of the sensor and the different bulk refractive index sensitivities of the TE and TM polarization are further emphasized in Fig. 5(c) where the phase shifts are plotted in the function of glycerol concentration for the two channels. The responses measured in the two channels are practically identical, emphasizing the excellent lateral homogeneity of the fabricated waveguides. Also, note that using a previously reported GCI configuration [49] a stable 2.1 10^{-5} rad/s drift was observed. We believe that the source of the recorded drift was the interaction of the waveguide material with the aqueous sample. Surface adsorption of ions, varying chemical group at the surface may slightly change the optogeometrical parameters of the waveguide film, causing a slowly saturating drift. In the present case, this type of drift is

#170857 - $15.00 USD Received 22 Jun 2012; revised 6 Sep 2012; accepted 7 Sep 2012; published 24 Sep 2012

eliminated by using a parallel sensing channel and internal referencing (see the difference signals in Fig. 5(a) and in Fig. 5(b)).

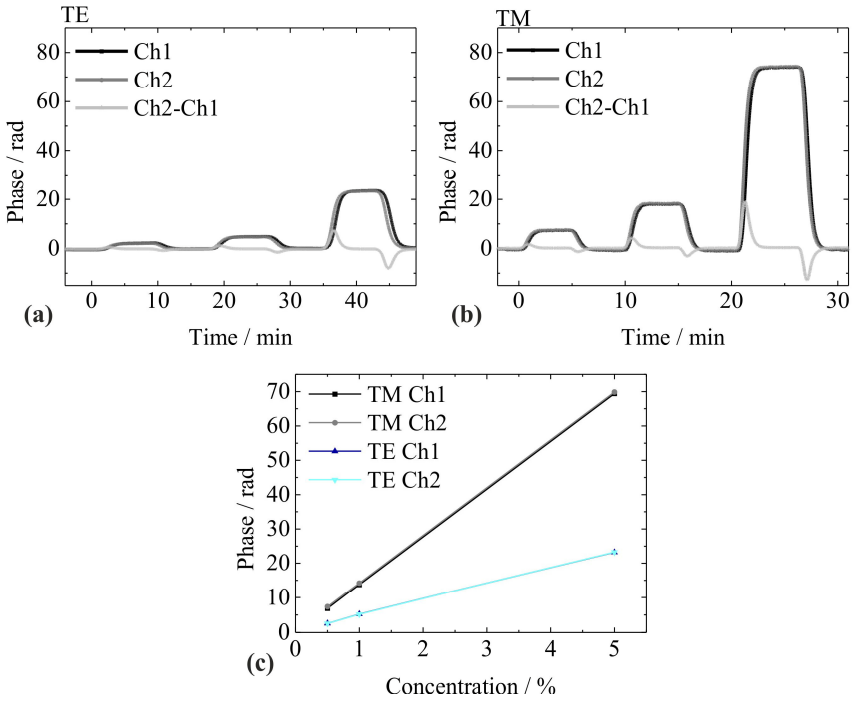

Fig. 5. Measured phase signals in the two channels when various glycerol solutions were flowed over the sensing areas. (a) TE polarization. (b) TM polarization. Since the channels are connected in series, the sample liquid flashes the Ch2 first and only after a short delay it arrives to Ch1. This causes the characteristic peaks and dips in the difference signals. (c) Linearity of the sensor for both polarizations.

3.4 Surface sensing - fibrinogen adsorption

In the next experiment, we investigated the surface sensitivities of the developed GCI configuration. In this case, the two fluidic channels were connected in parallel; giving the possibility to use Ch1 as an internal reference. First, pure buffer was flowed into both channels. After some time the pumped liquid was changed to fibrinogen solution in the fluidic line connected to Ch2. Figure 6 shows the monitored phase signals. The refractive index of the fibrinogen solution is $2x10^{-5}$ larger than the refractive index of the pure buffer. According to the sensitivity values earlier presented, this shift in refractive index causes a phase shift in the order of 0.1 rad. This value is negligible compared to the signals observed in Fig. 6. Therefore, the saturating signals in Fig. 6 are caused by the saturating protein adsorption on the surface of the waveguide. Injecting the buffer solution (see arrows in Fig. 6) some of the surface adsorbed proteins were washed off, decreasing the phase signal. Again, it is clearly seen that the TM configuration is more sensitive. It has an approximately 1.8 times more surface sensitivity, which is in good agreement with the calculations in Fig. 4 for the above mentioned thickness ranges of the waveguides. Taking the previously observed phase noise and assuming a refractive index of 1.46 for the molecules, the surface sensitivity of the device is estimated [49] to be below 0.1 pg/mm^2.

#170857 - $15.00 USD Received 22 Jun 2012; revised 6 Sep 2012; accepted 7 Sep 2012; published 24 Sep 2012

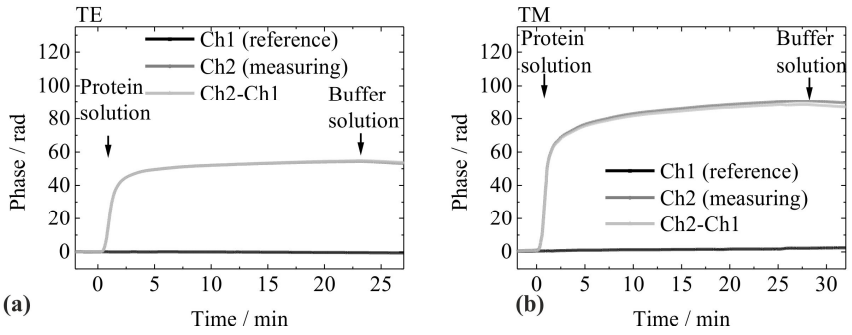

Fig. 6. Protein adsorption experiments. The arrows indicate the injection of the protein and buffer solutions into the fluidic channels. (a) TE polarization. (b) TM polarization.

4. Conclusions

In conclusion, a simple, low cost interferometric measurement configuration was developed for multichannel label-free sensing. The measurement arm of a conventional Mach-Zehnder interferometer was significantly miniaturized by replacing it with an integrated optical waveguide having two incoupling gratings. Refractive index variations close to the waveguide surface and between the incoupling gratings shift the phase in the measurement arm. Using a liquid crystal modulator at the free-space arm of the interferometer this phase shift was monitored in real time with excellent time resolution. In order to precisely control the mode interaction length and to optically seal the three grating regions from the sample the whole waveguide surface - except a 5 mm long area between the two incoupling gratings - was covered with a relatively thick layer of SiO_2.

As a further development, the interferometric signal is coupled out from the waveguide into the direction of the substrate at a 3rd grating area. The resulted measurement geometry is well suited for a wide range of applications; since it places the sample and fluidics above the waveguide sensor and all of the optics and interrogation units are positioned below the waveguide. The geometry is an excellent candidate for plate based multipoint screening (see refs. 43, 44) or lab on a chip applications, where parallel sensing units have to be miniaturized and space is critical (for example in handheld sensor devices)

The interrogation of the sensor was also performed in a novel way. Instead of illuminating the incoupling gratings with two parallel and coherent laser beams (as it is the case in conventional interferometry) an expanded laser beam was applied illuminating both incoupling gratings simultaneously. Using a two-cell LC modulator half of the beam was phase modulated in order to obtain the GCI signals. Thereby an alignment of the illuminating beams could be completely avoided and the interferometer became highly symmetrical, reducing its noise.

Another future advantage of the configuration is that the introduction of parallel sensing units is straightforward and easy. This was demonstrated by placing a two channel cuvette on top of the waveguide. Since the whole surface of the chip was homogeneously illuminated the channel O-rings not only defined the fluidic path, but at the same time created the sensing channels and effectively sealed one from another. This simplicity has especially great potential in miniaturized systems.

It was demonstrated that both TE and TM polarized waveguide modes can be applied in the new configuration. Their performances were compared both theoretically and experimentally. The resulting device was tested with liquid samples having different refractive indices and was applied for on-line monitoring the surface adsorption of fibrinogen. In the first set of experiments the two fluidic channels were connected in series, therefore channel to channel variations could be investigated. It was concluded that the sensor is capable of monitoring RI variations below 10^{-7} and without detectable discrepancy between the two channels. The later is due to the homogeneous illumination and proves that the

#170857 - $15.00 USD Received 22 Jun 2012; revised 6 Sep 2012; accepted 7 Sep 2012; published 24 Sep 2012

fabricated waveguides have excellent quality with very high lateral homogeneity. During the protein adsorption experiments the channels connected in parallel, using one of the channels for internal referencing, increasing the stability of the sensor. A protein surface coverage sensitivity of 0.1 pg/mm^2 was demonstrated. It is important to note that comparing this value with existing grating coupled optical waveguide technologies the sensitivity is two orders of magnitude better than of the widely used table top instrument using angular interrogation [22] or the compact wavelength interrogated sensor recently demonstrated [51].

The recent improvements demonstrate the suitability of the GCI system for highly sensitive label-free biochemical measurements. Based on the results obtained with the present configuration, a commercial instrument for highly sensitive monitoring of molecular interactions is being developed by Creoptix. Future potential applications include low cost point-of-care handheld testing devices for the areas of health, environmental or food.

Acknowledgment

Robert Horvath gratefully acknowledges the Reintegration Marie Curie Fellowship from the European Commission (OPTIBIO) and the Fellowship from the Hungarian Scientific Research Fund (OTKA PD). This work was supported by the National Development Agency grants TÁMOP-4.2.2/B-10/1-2010-0025 and REG_KD_09-2-2009-0022-NANOFLAG. This work was supported by the "Lendület" program of the HAS.

#170857 - $15.00 USD Received 22 Jun 2012; revised 6 Sep 2012; accepted 7 Sep 2012; published 24 Sep 2012